Journal of Alloys and Compounds 509 (2011) 1079–1083

Contents lists available at ScienceDirect

Journal of Alloys and Compounds

journal homepage: www.elsevier.com/locate/jallcom

# Synthesis, structure and optical properties of $CoAl_2O_4$ spinel nanocrystals

Xiulan Duan[a,*], Mei Pan[b], Fapeng Yu[a], Duorong Yuan[a]

[a] State Key Laboratory of Crystal Materials, Shandong University, 27 Shanda South Road, Jinan 250100, PR China
[b] School of Chemistry & Chemical Engineering, Sun Yat-Sen University, Guangzhou 510275, PR China

ARTICLE INFO

*Article history:*
Received 16 July 2010
Received in revised form
25 September 2010
Accepted 28 September 2010
Available online 8 October 2010

*Keywords:*
$CoAl_2O_4$ spinel
Sol–gel method
X-ray photoelectron spectroscopy
Optical properties

ABSTRACT

$CoAl_2O_4$ nanocrystals were synthesized by sol–gel method using citric acid as a chelating agent at low temperature. The as-synthesized samples were characterized by thermal analysis, X-ray powder diffraction, infrared spectroscopy and transmission electron microscopy. The results show that $CoAl_2O_4$ spinel is the only crystalline phase with a size of 10–30 nm in the temperature range 500–1000 °C. The temperature dependence of the distribution of $Al^{3+}$ and $Co^{2+}$ ions in the octahedral and tetrahedral sites in nanocrystals was investigated by X-ray photoelectron spectroscopy (XPS). It is observed that the inversion parameter decreases with increasing annealing temperature. Analysis of the absorption properties indicates that $Co^{2+}$ ions are located in the tetrahedral sites as well as in the octahedral sites in the $CoAl_2O_4$ nanocrystals. The origin of the green color (300–500 nm absorption band) should be due to the octahedrally coordinated $Co^{2+}$ ions.



## 1. Introduction

Spinel-type oxides $AB_2O_4$, where A and B stand for two different cations of comparable ionic sizes, are a class of chemically and thermally stable materials, which are suitable for a wide range of applications, such as magnetic materials, ceramics, and catalysis [1–4]. In the spinel structure, the oxygen ions form cubic close packed structure, and the A and B cations occupy two different crystallographic sites, tetrahedral and octahedral. The distribution of A and B cations in these two sites is affected by the combination and nature of the two cations and depends strongly on the preparation and processing conditions. Studies of cation distribution in spinels have attracted much attention because they may allow better understanding of the correlations between structure and properties such as color, diffusivity, magnetic behavior, catalytic activity and optical properties, which are strongly dependent on the occupation of these two sites by metals [5,6].

Among the class of materials, cobalt aluminate ($CoAl_2O_4$) spinel, known as Thenard's blue, is widely used as catalyst, color filter for automotive lamps or pigment layer on luminescent materials because of its thermal, chemical, photochemical stability and peculiar optical properties [7–12]. In recent years, much work has been done on the preparation and the optical properties of $CoAl_2O_4$ spinel materials [13–19]. A variety of techniques such as combustion [13], Pechini [14], sol–gel [15,17], and reverse microemulsion [16] have been successfully used for the preparation of cobalt aluminate oxide. Previous studies have shown that the color of $CoAl_2O_4$ is strongly affected by the synthesis temperature [17–19]. In more detail, the sample is green when synthesized at relatively low temperature, while it changes to blue when synthesized at relatively high temperature. At present, the origin of the green color of $CoAl_2O_4$ obtained at low temperature is still under debate. Some authors assigned the green color to the crystalline $Co_3O_4$ existing in $CoAl_2O_4$ spinel by referring to optical absorption measurements [19], while others thought it was related to the octahedrally coordinated $Co^{2+}$ ions in $CoAl_2O_4$ spinel [20,21]. To clarify this issue, we performed the structural investigations on nanocrystalline $CoAl_2O_4$ spinel.

X-ray photoelectron spectroscopy (XPS) is one of the most useful tools to get the structural information of nanocrystalline materials. It gives not only the chemical composition, but also the information on the chemical states of elements in the near surface region. Furthermore, the relative concentration of elements in different environments can be obtained by XPS analysis.

In this study, the pure nanocrystalline cobalt aluminate spinel was synthesized by the citrate sol–gel method. The evolution of the microstructure with changing annealing temperature was characterized by thermal analysis (TG/DSC), X-ray powder diffraction, infrared spectroscopy (IR) and transmission electron microscopy (TEM). The temperature dependence of the distribution of Al and Co cations in $CoAl_2O_4$ nanocrystals was studied by XPS. The relationship between the structure and the optical properties was also discussed.

* Corresponding author. Tel.: +86 531 88364864; fax: +86 531 88364864.
*E-mail address:* xlduan@sdu.edu.cn (X. Duan).

0925-8388/$ – see front matter © 2010 Elsevier B.V. All rights reserved.
doi:10.1016/j.jallcom.2010.09.199

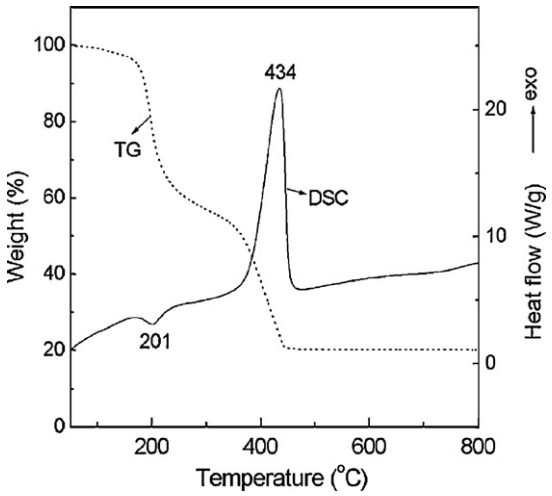


**Fig. 1.** DSC/TG curves of $CoAl_2O_4$ spinel precursor gel.

## 2. Experimental

### 2.1. Synthesis

Precursor sols of $CoAl_2O_4$ were prepared by a sol–gel technique using citric acid as a chelating agent. Firstly, a certain amount of cobalt nitrate ($Co(NO_3)_2{\cdot}6H_2O$) and aluminum nitrate ($Al(NO_3)_3{\cdot}9H_2O$) was dissolved in deionized water. Then proper amount of citric acid was added to the above solution with stirring. The molar ratio of metal ions to citric acid was 1:2. The mixed solution was stirred for 1 h and then heated in an 80 °C water bath until a highly viscous gel was formed. The pink gels were dried in oven at 110 °C and then fired to the desired temperatures (500–1000 °C) for 5 h.

### 2.2. Characterization

Thermogravimetry (TG) and differential scanning calorimetry (DSC) analyses of the precursor were performed using a DSC/TGA analyzer (Model Q600 SDT) in flowing nitrogen atmosphere with a heating rate of 10 °C/min. The X-ray diffraction (XRD) patterns of the obtained powders were carried out by a Japan Rigaku D/Max-rA diffractometer using a Cu-target tube ($\lambda$ = 0.15418 nm) and a graphite monochromator. Fourier transform infrared (FT-IR) spectroscopy was conducted with a Nicolet 750 spectrometer. The morphology and the size of nanocrystalline $CoAl_2O_4$ after heating at 500–900 °C for 5 h were observed by transmission electron microscopy (TEM) (JEM-100CXII).

X-ray photoelectron spectra were measured using an ESCALAB 250 spectrometer with monochromatized Al $K_\alpha$ X-ray radiation in ultrahigh vacuum ($<10^{-7}$ Pa). The binding energies were calibrated by taking C 1s peak (284.6 eV) of adventitious carbon as reference. The peaks were deconvoluted after background subtraction, using a mixed Gaussian–Lorentzian function. Fractional atomic concentrations of the elements were calculated using empirically derived atomic sensitivity factors [22]. Diffuse absorbance spectra after Kubelka–Munk transformation, were recorded with a step of 1 nm on a Varian Cary5000 spectrophotometer using an integration sphere at room temperature. Polytetrafluoroethene was used as reference.

## 3. Results and discussion

The TG/DSC curves of the dried gel are shown in Fig. 1. The endothermic peak at 201 °C is due to the decomposition of nitrates, accompanied by significant weight loss. The exothermic peak at 434 °C corresponds to the crystallization of the $CoAl_2O_4$ spinel. There is no distinct weight loss at temperature higher than 450 °C.

Fig. 2 shows XRD patterns of the $CoAl_2O_4$ gels annealed at 500–1000 °C for 5 h. Several diffraction peaks are observed in the patterns and the position of these peaks closely resembles that of cubic $CoAl_2O_4$ spinel (JCPD Card No. 10-458), indicating the formation of cobalt aluminate phase. The presence of spinel phase is also confirmed by the appearance of the weak peak at about $2\theta = 49°$ (331), which is characteristic for the $CoAl_2O_4$ phase. The intensity of the diffraction peaks increases with increasing annealing temperature, which is associated with an increase in crystallinity. By means of the Scherer formula, an average grain size of the particles was

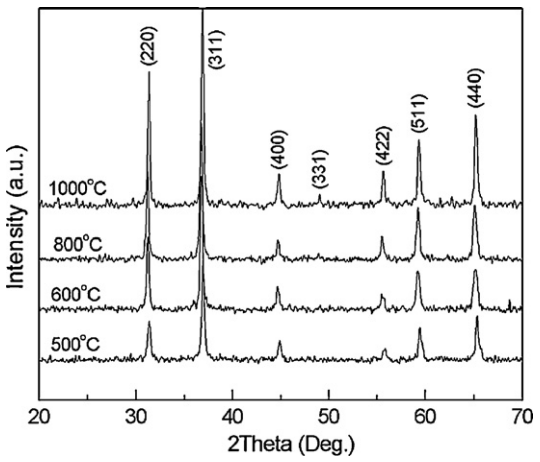


**Fig. 2.** XRD patterns of $CoAl_2O_4$ nanocrystals annealed at different temperatures.

**Table 1**
Particle size of $CoAl_2O_4$ nanocrystals obtained from XRD and TEM.

| Annealing temperature (°C) | Particle size (nm) | |
|---|---|---|
| | XRD | TEM |
| 500 | 10.5 | 10 |
| 600 | 16 | 17 |
| 800 | 24 | 25 |
| 900 | | 27 |
| 1000 | 30 | |

calculated to be 10–30 nm in the temperature range 500–1000 °C and shown in Table 1.

The IR spectra of the annealed samples at 500 and 800 °C are shown in Fig. 3. Several peaks are observed at around 670, 555 and 501 $cm^{-1}$, respectively, which indicates the formation of $CoAl_2O_4$ spinel [17]. The broad absorption peak at 3413 $cm^{-1}$ is assigned to the vibration modes of metal attached hydroxyl groups. The peak at 1626 $cm^{-1}$ represents the stretching vibrations of carboxyl groups ($COO^-$) of citrate ions complexed to the metal ions in polymetric intermediates. The two peaks at 1401 and 1516 $cm^{-1}$ are related to $NO_3-$ ions [23]. As the heat-treatment temperature increased, the peaks related to $CoAl_2O_4$ became stronger, indicating the growth of nanocrystals.

The TEM micrographs of the samples annealed at 500–900 °C are shown in Fig. 4. The micrographs indicate that an average size

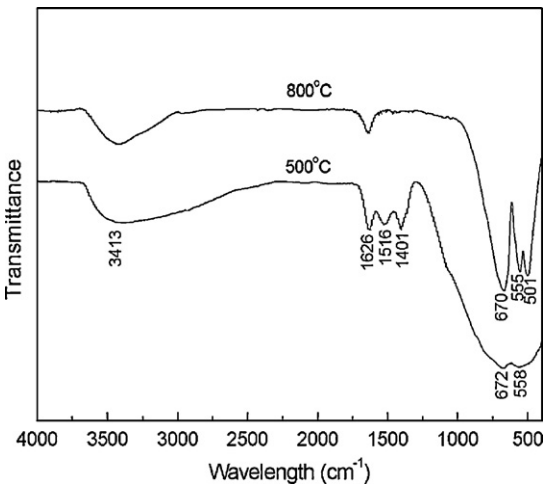


**Fig. 3.** IR spectra of $CoAl_2O_4$ nanocrystals.

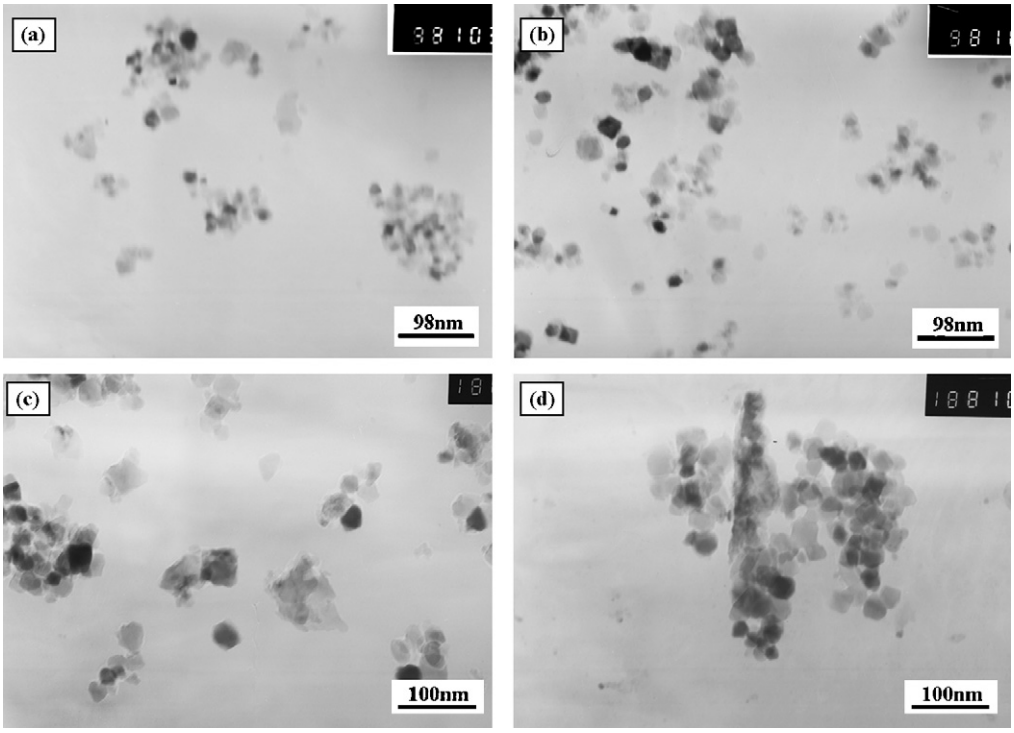


**Fig. 4.** TEM images of $CoAl_2O_4$ nanocrystals heated at different temperatures: (a) 500 °C; (b) 600 °C; (c) 800 °C; and (d) 900 °C.

**Table 2**
XPS data for Al 2p spectra of $CoAl_2O_4$ nanocrystals annealed at different temperatures.

| Temperature (°C) | Binding energy (eV) | Area ratio | FWHM (eV) | L/G (%) |
|---|---|---|---|---|
| 600 | 74.14 | 1.0 | 1.85 | 30 |
| | 73.26 | 0.17 | 1.85 | 30 |
| 800 | 74.14 | 1.0 | 1.85 | 30 |
| | 73.26 | 0.14 | 1.85 | 30 |
| 1000 | 74.14 | 1.0 | 1.85 | 30 |
| | 73.26 | 0.12 | 1.85 | 30 |

**Table 4**
Reference XPS data for O 1s and Co 2p (eV).

| Compound | Co $2p_{3/2}$ | O 1s | Refs. |
|---|---|---|---|
| Co | 778.2 | | [24,25] |
| CoO | 780.4 | 530.1 | [26] |
| $Co_2O_3$ | 780.5 | 529.9 | [27] |
| $Co_3O_4$ | 779.7 | 530.2 | [26] |
| | 780.9 | 529.7 | [28] |
| $CoAl_2O_4$ | 781.4 | 531.3 | [34] |
| | 781.7 | | [31] |
| | 781.8 | | [32] |

of the $CoAl_2O_4$ nanocrystalline particles is 10–30 nm in diameter, which is consistent with the XRD analysis (Table 1). When the heat-treatment temperature was increased to 900 °C, the particles tend to agglomerate.

The survey XPS spectrum of $CoAl_2O_4$ nanocrystals annealed at 1000 °C indicates that no other elements were detected except for the original components and contaminated carbon (as shown in Fig. 5a). The C 1s peak at 284.6 eV of contaminated carbon was used as reference. The high-resolution photoelectron spectra of Al 2p, Co 2p and O 1s for the samples annealed at 600–1000 °C are displayed in Fig. 5b–d, respectively. The quantitative XPS data for Al 2p spectra are shown in Table 2. The binding energies (BE) of Co, Al and O core levels of the as-synthesized nanocrystals are listed in Table 3. For comparison, the XPS data of cobalt-containing reference materials are listed in Table 4 [24–28].

According to the report by Pawlak in 1999, the Al 2p binding energies of octahedral and tetrahedral $Al^{3+}$ ions are at 74.13 and 73.26 eV, respectively [29]. In our experiment, the Al 2p binding energy of all annealed samples are in this region, which indicates that the $Al^{3+}$ ions occupy these two different sites in $CoAl_2O_4$ nanocrystals. As shown in Fig. 5c, the Al 2p spectra are deconvoluted into two peaks using the octahedral and tetrahedral $Al^{3+}$ BE values of 74.13 and 73.26 eV, respectively. The detailed deconvolution parameters are shown in Table 2. The octahedral $Al^{3+}$ ions are dominant in nanocrystals. Based on the result, we think that the as-prepared $CoAl_2O_4$ nanocrystals are partially inversed spinel-structure. The inversion parameter $x$, is defined as the fraction of $Co^{2+}$ ions in octahedral sites (or two times the fraction of $Al^{3+}$ ions in tetrahedral sites). Taking account of cation distributions, the formula of the compound can be written as $(Co_{1-x}Al_x)[Co_xAl_{2-x}]O_4$,

**Table 3**
Binding energies of Co 2p, O 1s, Al 2p core level (eV) and inversion parameter ($x$) of $CoAl_2O_4$ nanocrystals annealed at different temperatures.

| Temperature (°C) | Co $2p_{3/2}$ | Co $2p_{1/2}$ | O 1s | Al 2p (percentage of overall Al 2p peak areas %) | | $x$ |
|---|---|---|---|---|---|---|
| 600 | 781.74 | 797.24 | 531.5 | 74.14 | (85.5) | 0.29 |
| | | | | 73.26 | (14.5) | |
| 800 | 781.94 | 797.44 | 531.5 | 74.14 | (87.8) | 0.24 |
| | | | | 73.26 | (12.2) | |
| 1000 | 781.98 | 797.48 | 531.5 | 74.14 | (89.3) | 0.21 |
| | | | | 73.26 | (10.7) | |

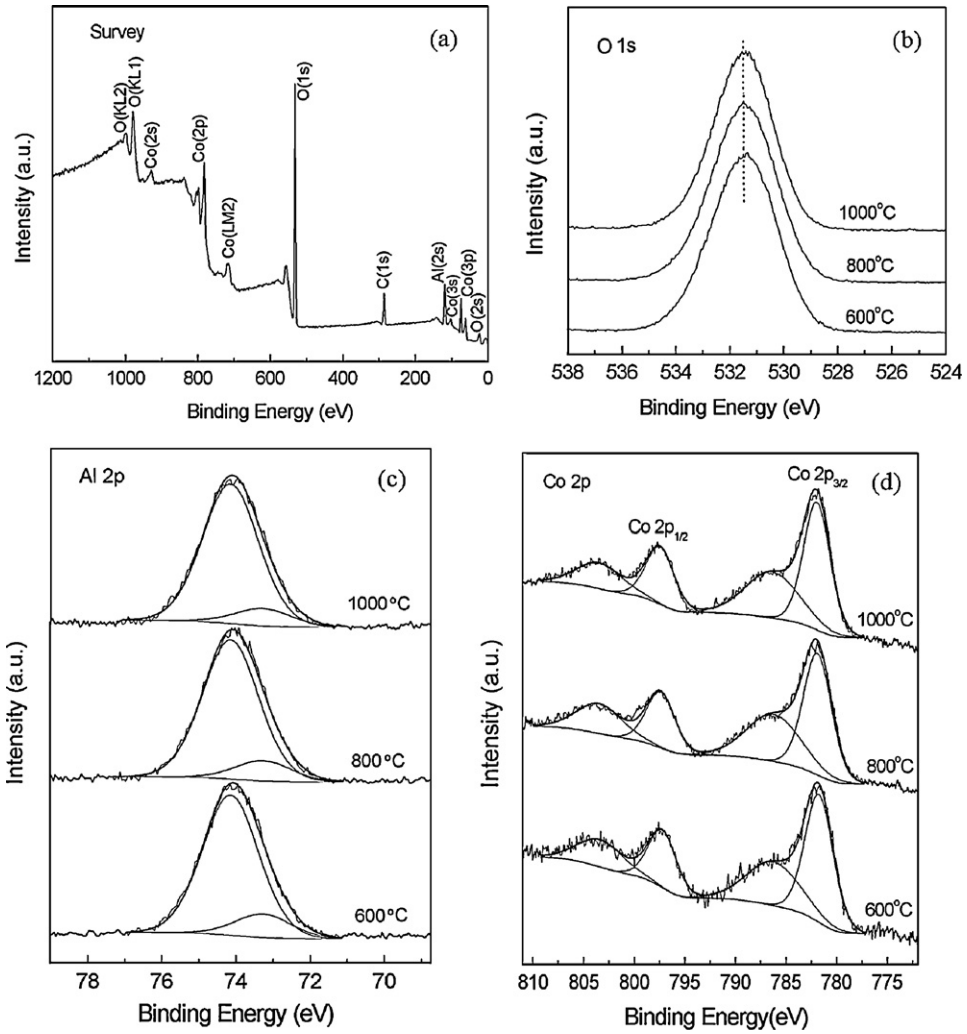


**Fig. 5.** Survey XPS spectrum of the as-prepared $CoAl_2O_4$ nanocrystals annealed at 1000 °C (a), and XPS spectra of (b) O 1s, (c) Al 2p, (d) Co 2p core levels of $CoAl_2O_4$ nanocrystals at different heat-treatment temperatures.

where parentheses and square brackets denote the tetrahedral and octahedral sites, respectively. The parameter $x$ can be estimated according to the area ratio of the two peaks, which correspond to the tetrahedral and octahedral $Al^{3+}$ ions, and the result is shown in Table 3. It can be seen that the $x$ value is 0.29 for the nanocrystals annealed at 600 °C, and decreases to 0.21 when the annealing temperature is 1000 °C. The change of the inversion parameter with increasing annealing temperature is consistent with the latest report [30]. The result indicates that the amount of $Al^{3+}$ ions in the tetrahedral sites decreases with increasing heat-treatment temperature.

The Co 2p core level spectra of $CoAl_2O_4$ nanocrystals at different heat-treatment temperatures show peaks at $781.86 \pm 0.12$ eV with the broad satellite around 786.5 eV, and $797.36 \pm 0.12$ eV with the satellite around 803 eV, which are due to Co $2p_{3/2}$ and Co $2p_{1/2}$, respectively. The Co $2p_{3/2}$ values are similar to those reported by Zsoldos and Guczi [31] (781.7 eV) and Chung and Masslth [32] (781.8 eV). There is no peak at around 780 eV, which indicates the absence of $Co_2O_3$ or $Co_3O_4$ phases. The peaks and their intense shake-up satellites are typical for divalent high spin cobalt [33]. However, the Co $2p_{3/2}$ peak with the fwhm of ~3.4 eV is rather broad. Based on the above analysis, the structure of $CoAl_2O_4$ nanocrystals is partially inversed. Therefore, the broad peak should arise from the distributions of $Co^{2+}$ ions over tetrahedral and octahedral sites. The binding energy of Co $2p_{3/2}$ slightly increases with increasing annealing temperature, indicating that the relative amount of $Co^{2+}$ ions in tetrahedral sites increases and the inversion parameter decreases. The O 1s signals show symmetric and only one peak at 531.5 eV for all the annealed samples (Fig. 5b). The binding energy value of O 1s is similar to that of O in bulk $CoAl_2O_4$ reported by Patterson et al. [34], which is 531.3 eV when C 1s of 284.6 eV was used as reference.

To study the correlation between cation distribution and optical properties of $CoAl_2O_4$ nanocrystals, we measured the diffuse absorption spectra of the samples annealed at 800–1000 °C. Fig. 6a shows the absorption spectrum of 800 °C-annealed sample in the wavelength range 250–1900 nm. The intense absorption peak at 600 nm and the broad band centered at 1400 nm are characteristic of $Co^{2+}$ ions in tetrahedral sites in crystalline materials [35,36]. The peak at 600 nm is assigned to the $^4A_2(^4F) \rightarrow {}^4T_1(^4P)$ transition and the broad absorption band in the near-infrared is assigned to the $^4A_2(^4F) \rightarrow {}^4T_1(^4F)$ transition of tetrahedrally coordinated $Co^{2+}$ ions. In addition, an absorption band at 300–500 nm appears in the spectrum. With regard to the above discussions and the cation distribution previously characterized, this new band, leading to a green color, could be due to the $Co^{2+}$ ions in octahedral sites. The similar band generated by octahedrally coordinated $Co^{2+}$ has been reported by other authors [37,38]. The intensity of the absorption band at 300–500 nm decreases with the increase of the heat-treatment temperature (Fig. 6b). This is because the frac-

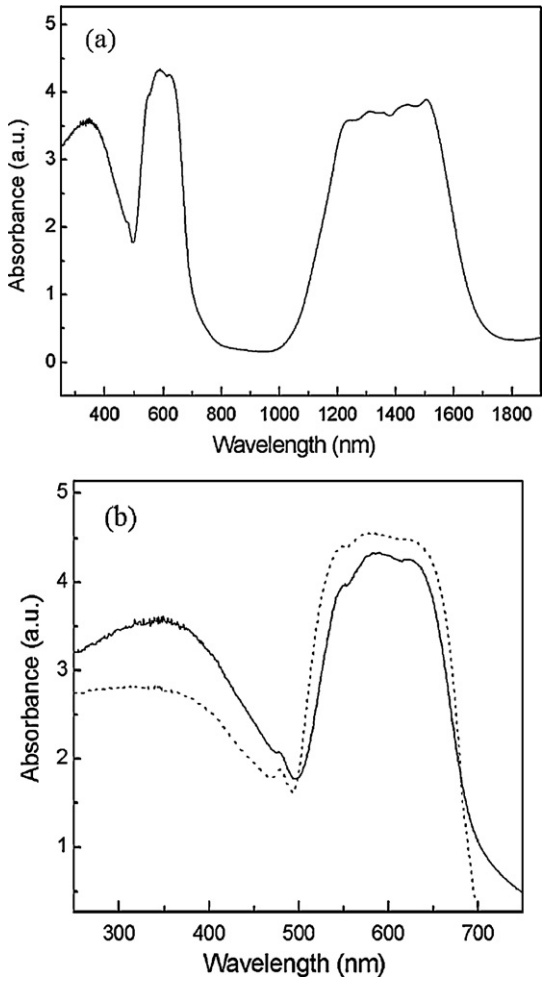


**Fig. 6.** Absorption spectra of (a) $CoAl_2O_4$ nanocrystals annealed at 800 °C in the wavelength range 250–1900 nm, (b) $CoAl_2O_4$ nanocrystals annealed at 800 °C (solid curve) and 1000 °C (dot curve) in the wavelength range 250–750 nm.

tion of octahedrally coordinated $Co^{2+}$ ions decreases. Based on the above discussion, it is confirmed that the origin of the green color (300–500 nm band) is related to the octahedrally coordinated $Co^{2+}$ ions of the $(Co_{1-x}Al_x)[Co_xAl_{2-x}]O_4$ nanocrystalline structure.

## 4. Conclusions

Pure $CoAl_2O_4$ nanocrystals with a size of 10–30 nm have been synthesized by the citrate sol–gel method. The coordinative environment of aluminum and cobalt ions in $CoAl_2O_4$ nanocrystals has been investigated by XPS. The $Al^{3+}$ and $Co^{2+}$ ions occupy both octahedral and tetrahedral sites in nanocrystalline structure. The as-synthesized $CoAl_2O_4$ nanocrystals are partially inverted spinel and the inversion parameter decreases with the increasing annealing temperature. The optical properties of the nanocrystals are discussed based on the structural results. The 300–500 nm absorption band, responsible for the green color, is related to the octahedrally coordinated $Co^{2+}$ ions of the $(Co_{1-x}Al_x)[Co_xAl_{2-x}]O_4$ crystalline phase.

## Acknowledgment

This work was supported by a grant from the National Natural Science Foundation of China (50902089).

## References

[1] I.H. Gul, A. Maqsood, M. Naeem, M. Naeem Ashiq, J. Alloys Compd. 507 (2010) 201.
[2] F. Tielens, M. Calatayud, R. Franco, J.M. Recio, M. Perez-Ramirez, C. Minot, J. Phys. Chem. B 110 (2006) 988.
[3] N. Ballarini, F. Cavani, S. Passeri, L. Pesaresi, A.F. Lee, K. Wilson, Appl. Catal. A: Gen. 366 (2009) 184.
[4] M. Sakavatu-Niasari, F. Davar, Mater. Lett. 63 (2009) 441.
[5] I.B. Bersuker, Electronic Structure and Properties of Transition Metal Compounds, John Wiley & Sons, New York, 1996.
[6] R. Burns, Mineralogical Applications of Crystal Field Theory, vol. 5, Cambridge University Press, Cambridge, 1993.
[7] C. Maurizio, N. El Habra, G. Rossetto, M. Merlini, E. Cattaruzza, L. Pandolfo, M. Casarin, Chem. Mater. 22 (2010) 1933.
[8] A. Walsh, Y. Yan, M.M. Al-Jassim, S.-H. Wei, J. Phys. Chem. C 112 (2008) 12044.
[9] X.L. Duan, D.R. Yuan, Z.H. Sun, C.N. Luan, D.Y. Pan, D. Xu, M.K. Lv, J. Alloys Compd. 386 (2005) 311.
[10] P.M.T. Cavalcante, M. Dondi, G. Guarini, M. Raimondo, G. Baldil, Dyes Pigments 80 (2009) 226.
[11] W.S. Cho, M. Kakihana, J. Alloys Compd. 287 (1999) 87.
[12] D. Rangappa, T. Naka, A. Kondo, M. Ishii, T. Kobayashi, T. Adschiri, J. Am. Chem. Soc. 129 (2007) 11061.
[13] T. Mimani, J. Alloys Compd. 315 (2001) 123.
[14] L. Gama, M.A. Ribeiro, B.S. Barros, R.H.A. Kiminami, I.T. Weber, A.C.F.M. Costa, J. Alloys Compd. 483 (2009) 453.
[15] F.L. Yu, J.F. Yang, J.Y. Ma, J. Du, Y.Q. Zhou, J. Alloys Compd. 68 (2009) 443.
[16] J. Chandradass, M. Balasubramanian, K.H. Kim, J. Alloys Compd. 06 (2010) 395.
[17] M. Zayat, D. Levy, Chem. Mater. 12 (2000) 2763.
[18] I.S. Ahmed, S.A. Shama, M.M. Moustafa, H.A. Dessouki, A.A. Ali, Spectrochim. Acta A 74 (2009) 665.
[19] U.L. Stangar, B. Orel, M.J. Krajnc, J. Sol-Gel Sci. Technol. 26 (2003) 771.
[20] H.S.C. O'Neill, Eur. J. Mineral. 6 (1994) 603.
[21] A. Natasuka, Y. Ikda, Y. Yamasaki, N. Nakayama, T. Mizota, Solid State Commun. 128 (2003) 85.
[22] C.D. Wagner, L.E. Davis, M.V. Zeller, J.A. Taylor, R.M. Raymond, L.H.G. Gale, Surf. Interface Anal. 3 (1981) 211.
[23] D.L. Wei, Z.L. Jia, K.G. Jing, J. Eur. Ceram. Soc. 23 (2003) 2289.
[24] J. Habe, L. Ungier, J. Electron Spectrosc. Relat. Phenom. 12 (1977) 305.
[25] R.B. Moyes, M.W. Roberts, J. Catal. 49 (1977) 216.
[26] V.I. Nefedov, D. Gaii, B.F. Dzhurinskii, N.P. Sergushin, Y.V. Salyn, Zh. Neorg. Khim. 20 (1975) 2307.
[27] N.S. Mclniyre, M.G. Cook, Anal. Chem. 47 (1975) 2208.
[28] P. Gajardo, D. Pirotte, C. Defosse, P. Grange, B. Delmon, J. Electron Spectrosc. Relat. Phenom. 17 (1979) 121.
[29] D.A. Pawlak, K. Woźniak, Z. Frukacz, T.L. Barr, D. Fiorentino, S. Seal, J. Phys. Chem. B 103 (1999) 1454.
[30] M. Gaudon, A. Apheceixborde, M. Menetrier, A. Le Nestour, A. Demourgues, Inorg. Chem. 48 (2009) 9085.
[31] Z. Zsoldos, L. Guczi, J. Phys. Chem. 96 (1992) 9393.
[32] K.S. Chung, F.E. Masslth, J. Catal. 64 (1980) 320.
[33] D. Briggs, M.P. Seah, Practical Surface Analysis, vol. 1, 2nd ed., Wiley, New York, 1993.
[34] T.A. Patterson, J.C. Carver, D.E. Leyden, D.M. Hercules, J. Phys. Chem. 80 (1976) 1702.
[35] T. Abritta, F.H. Blak, J. Lumin. 48&49 (1991) 558.
[36] J. Ferguson, D.L. Wood, L.G. Van Uitert, J. Chem. Phys. 51 (1969) 2904.
[37] S. Cava, S.M. Tebcherani, S.A. Pianaro, C.A. Paskocimas, E. Longo, J.A. Varela, Mater. Chem. Phys. 97 (2006) 102.
[38] F. Matteucci, G. Cruciani, M. Dondi, G. Gasparotto, D.M. Tobaldi, J. Solid State Chem. 180 (2007) 3196.